Influence of Rock Alteration in Carbonates by CO_2 Injection, on Reservoir and Geomechanical Integrity of a Carbon Capture and Storage Unit

Syed A. Islam[1]

[1]slb

Extended abstract

Background

This paper describes the influence of rock alteration from CO2 injection in a carbonate reservoir on the geomechanical integrity of the storage unit. If the injection pressures are higher than the rock breakdown pressures, the reservoir and/or caprock can fracture and the injected CO2 can migrate to unwanted areas. Secondly, the injection process can alter the state of stress along faults, potentially destabilizing it and causing migration of injected CO2 to the overlying strata. Thirdly, in case of poor well cementing, the injected fluid can again migrate to unwanted areas through cement channels. First two risks are assessed through coupled reservoir-geomechanics simulations, which is discussed here. Upon entering the reservoir, the injected CO2 will react with formation brine and will create a weak carbonic acid, which will react with the carbonate minerals in rock altering its petrophysical and geomechanical properties. Porosity and permeability will alter along with rock elastic and strength properties. This can alter the state of stress in the reservoir and caprock and has the potential to cause containment breach causing CO2 leak.

This paper discusses the methodology of coupled reservoir-geomechanics simulation on asynthetic model [1]. The model loosely represents the Kharib formations in the giant onshore fields in Abu Dhabi. Field development and production follows the life cycle of a real field. Oil is produced from the 200 producers and injector through water flooding for 50 years. After the pressures have depleted, the CO2 pilot project is implemented in the central crest using 12 injectors and 12 producers. Oil is produced for another 30 years through CO2 EOR. After this the production is stopped and CO2 is injected for 100 years followed by monitoring of CO2 plume for 500 years.

The simulation is implemented through coupling the ECLIPSETM and VISAGETM for reservoir and geomechanics simulations respectively. The pressure and saturation data are passed from reservoir to geomechanics simulator which computes stresses and strains. The reservoir simulator keywords are used to alter petrophysical properties at selected time steps, to account for rock alteration from CO2 reactions. The stresses and strains are used to assess the geomechanical integrity of reservoir through applying a Mohr-Coulomb failure criteria.

Introduction

A suitable site for CO2 requires certain criteria to be fulfilled for CO2 to be contained in reservoir for long time [2]. For example, the reservoir needs to be deeper than 1000 m, in a low tectonic activity area, limited to moderate faults and should have at least one major regional seal. These criteria are easily fulfilled by giant carbonate fields in Middle East, which are thus an attractive proposition for CO2 storage once

depleted. However, concern regarding dissolution of carbonate minerals in injected CO2 solution can be a concern. The injected CO2 dissolves quickly in water producing a weak carbonic acid lowering the pH of formation brine [3],

$$CO2 + H2O \text{ ----> } H2CO3 \text{ ----> } H+ + HCO3- . \quad (1)$$

This initiates further reactions which dissolves carbonate minerals from the rock matrix,

$$H+ + HCO - + CaCO\ (s) \text{ <----> } Ca2+ + 2HCO - , \quad (2)$$
$$H+ + HCO - + MgCO\ (s) \text{ <----> } Mg2+ + 2HCO -, \quad (3)$$
$$H+ + HCO - + FeCO\ (s) \text{ <----> } Fe2+ + 2HCO - , \quad (4)$$

where the subscript (s) stands for solid phase. The dissolution of rock minerals alters the porosity, permeability, elastic properties, and rock strength. Most of the lab results conducted on core plugs saturated with injected CO2 solution report an increase in porosity with time, however the effect on permeability is mixed. Normally the enhancement in porosity should results in permeability increase, however in some cases the dissolved minerals can re-precipitate which can block pore throats to reduce permeability. More rock dissolution occurs in heterogeneous rocks than homogeneous ones. Pokrovsky et al [4] report that dolomite and magnesite type of rocks exhibit dissolution rates at least ten times or even slower than calcite rock. In a vuggy formation the reaction is likely to create localized permeable pathways, commonly called wormholes. Luqot et al [5] reports that wormholes are likely to be created at high injection pressures, whereas at low injection pressures the carbonate is expected to dissolve uniformly. However, it must be noted that in practical field conditions such an alteration is highly likely to remain confined near the injection point, as reported by Smith et al [6] from Weyburn project in Canada. This is because the pH of aqueous solution will stabilize and increase quickly away from the wellbore as most of the H+ cations are used up in dissolving carbonate minerals. Saaltink et al [7] observe through numerical simulations that porosity enhancement due to CO2 injection near well is small, due to low solubility of calcite. Once the CO2 concertation reaches saturation within brine, the dissolution reactions slow down considerably, and the porosity does not increase any further. Due to this reason, the porosity enhancement only occurs at the plume front. The brine below the plume has already reached saturation and further porosity enhancement is not possible.

Modeling effect of mineral dissolution

Several researchers have reported results of mineral dissolution on petrophysical properties. Zaree et al [8] reports permeability increases by 400 times of initial permeability after 57 PV (pore volume) flooding in a case from Zagros core plug where the mineral was strongly soluble in acid. Lamy-Chappius et al [9] report porosity increases in the range of 5-15% from dissolution of calcite rich sandstone and an increase in permeability in the range of 50-75%.

Smith et al [10] presented and validated a reactive transport model for predicting the porosity and permeability changes in carbonates core samples. Based on their experiments they present a reactive transport model,

$$Rm = -S * k298K * e\ (-E/R) * (1/T - 1/298K) * (1 - Q/Keq) , \quad (5)$$

where, Rm is mole dissolving in units of mole/m^2s, S is reactive surface area of the respective mineral phase in m^2, k298K is mineral specific rate constant determined at 298K (25°C), E is mineral specific activation energy in kJ/mol, R is universal gas constant in kJ/mol-K, T is temperature in K, Keq is mineral specific equilibrium constant at the temperature of interest, and Q is the ion activity product. The right- hand parenthesis ties the kinetic rate of the reaction to fluid-mineral saturation, such that Rm slows to zero when Q = Keq at chemical equilibrium. If Q < Keq, mineral dissolution continues by undersaturated condition. Q > Keq indicates supersaturate condition where reverse reaction occurs and mineral precipitates.

Rate of change in mineral volume from dissolution is described by,

$$\frac{d\theta_m}{dt} = R_m . V_m \qquad (6)$$

where, $Vm$is specific molar volume of the reactive carbonate mineral m and $\partial\theta m$ is the change in mineral volume.
Finally, the change in resulting porosity is given by,

$$\frac{d\emptyset_m}{dt} = -\Sigma \frac{d\theta_m}{dt} \qquad (7)$$

Thus, the porosity change is the sum of change in individual mineral volumes through dissolution. Negative sign indicates that as the mineral volume decreases, the porosity increases.

Implementing Chemical reactivity in available simulators

Currently the availability of proper chemical-reservoir-geomechanical coupled simulator is limited. In academia TOUGHREACT is a comprehensive multi-component reactive fluid flow simulator, however it is not suitable for use in large oil and gas fields. Computer Modeling Group's GEM simulator is supposed to have this capacity; however, the author did not have the access to it. For this work, commercially available compositional reservoir simulator ECLIPSE-300 is used which is a common compositional simulator in industry. The simulator is run in "CO_2SOL" mode which is suitable for CO_2 EOR (enhanced oil recovery) and storage in a depleted oil reservoir. One limitation of running in this mode is that the reprecipitation of solids in brine is not available.

The alteration of porosity from CO_2 injection is handled through Keywords. Only porosity enhancement is modelled, and the results are compared with no porosity enhancement case. The porosity enhancement is done only in the injector cells, to mimic the case that porosity is altered only near wellbore as discussed above. An extreme case is also modelled whereby porosity is altered in a bigger zone. Mechanical properties are also altered through linear functions against CO_2 mole fraction. The porosity enhancement will make the carbonate rocks weaker and the properties like the Young's modulus and UCS will decrease. This is implemented through a function whereby the properties such as Young's modulus decrease with CO_2 mole fraction, as shown in Figure 1.

Coupling between reservoir and geomechanics simulators

Commercial finite element geomechanics simulator VISAGE is used for computing stress and strain. The input to VISAGE is a 3D structural model, populated with mechanical and petrophysical properties and pore pressure. The mechanical properties include elastic properties like Young's modulus, Poisson's Ratio and Biot constant; strength properties like Unconfined Compressive Strength (UCS), Friction Angle and Tensile strength, and properties to model plastic behavior like Dilation angle and Hardening coefficient. Petrophysical properties include porosity and bulk density. The pore pressure at any time step is passed from reservoir to geomechanics simulator. The geomechanical simulator runs and calculates stresses and strains at different points in the structure. As the pore pressure changes, the stresses acting in the reservoir changes, and the pore volume changes due to compressibility. In addition, the pore volume also changes from chemical alteration on reaction with CO_2. The change in pore volume is used to compute change in permeability through using the power law.

$$\frac{k_t}{k_o} = \left(\frac{\emptyset_t}{\emptyset_o}\right)^n \quad (8)$$

where, k_t is Permeability at time t, ko is initial permeability, ϕ_t is porosity at time t, ϕ_o is initial porosity and 'n' is a constant, generally 3. The change in porosity and permeability computed by geomechanics simulator is passed on to reservoir simulator which uses these in next step. During CO_2 injection, the CO_2 mole fraction computed from reservoir simulator is also passed to geomechanics so that it can alter the rock mechanical properties to mimic the rock alteration with CO_2 injection. Such a two-way coupling scheme is shown in Figure 2.

Model Setup

The original synthetic model is 140 x 80 km as shown on the left-hand side in Figure 3. The model consists of three main anticlines representing multiple closures. This project is done on a part of the central anticline bounded by red square and shown on the right. The selected part represents a carbonate platform from Early Cretaceous/Aptian age.

The structure is suitable for CO_2 storage as it is a gentle anticline, with four-way closure and little to none faults. The reservoir is overlain by thick regional Nahr Umr shale and very tight Maudud carbonates. The reservoir consists of fifteen zones which are divided into sixty-two layers. Porosity is 20% or higher and permeability ranges from 15 to 600 mD. Top thirty-two layers have a higher permeability, and these are perforated for production. CO_2 is injected in the bottom thirty layers having lower permeability to avoid fingering. Reservoir is undersaturated, medium light oil with no GOC. Petrophysical properties vary a lot in carbonates and for this reason the reservoir is divided into different rock types based on the unique porosity-permeability relationship, and capillary pressure curves exhibited, which in turns is a representation of the rock depositional and subsequent diagenesis. The relative permeability curves of the three facies are given in Figure 4. PVT data of the reservoir fluid is listed in Table 1.

Table 1. PVT data of the reservoir fluid.

Gas gravity	0.75	w.r.t air
Oil gravity	42	API
Oil density	50.9	lb/ft3
Water density	65.34	lb/ft3
Bubble Point pressure	2200	psi
Water salinity	157482	ppm
Initial Pressure	4534	psi
Datum Depth	7900	ft TVDSS
Oil Water	8080	ft TVDSS
Gas oil Contact	7170	ft TVDSS
Pc at OWC	~0	psi
Pc at GOC	N/A	
Temperature	240	°F
Oil FVF	1.412	bbl/STB
Water FVF	1.06	bbl/STB

Geomechanical Model

For geomechanical simulation the overburden layers are added including the caprock Nahr Umr and Maudud carbonates. Some layers are added in the bottom also. **Figure 5** shows the 3D structure of geomechanical simulation. The elastic and strength properties are determined from log data and using correlations typically used in the region. **Table 2** lists the average geomechanical properties of different formations. The stresses are determined using the poroelastic model. The lower limit of fracture gradient in the reservoir was close to 0.7 psi/ft, based on which the BHP in injectors was limited to 5000 psi. Direction of maximum horizontal stress is taken as N25°E, based on published data [11]. **Table 3** shows the schedule used for simulation.

For simulation purposes CO2SOL algorithm of ECLIPSE is used which is suitable for CO_2 injection in oil reservoirs. The reservoir and geomechanical simulators are coupled as described above. ECLIPSE pressure and CO_2 concentration are passed on to VISAGE. The volumetric strain in reservoir from pressure and stress changes is used to compute the change in porosity and permeability and is passed back to ECLIPSE. In addition, keywords MULTPV, MULTX, MULTY and MULTZ are used to simulate the alteration of rock properties with CO_2 injection. Porosity is enhanced by 10% near wellbore total, after 10 years of CO_2 injection.

Table 2. Average mechanical properties computed for different formations.

	Poisson's ratio	Young's Modulus	Unconfined Compressive Strength (UCS)	Tensile Strength	Friction Angle	Bulk Density	Biot's Alpha
	unitless	Mpsi	psi	psi	deg	g/cc	unitless
UER	0.3	1.32	5601	560	25.7	2.35	1
SIMSIMA	0.3	3.28	13894	1390	32.6	2.46	1
LAFFAN	0.3	1.96	8325	465	27.9	2.44	1
MISHRIF	0.3	1.88	7985	798	27.7	2.58	1
MAUDUD	0.3	3.25	13771	1377	32.5	2.40	1
Nahr Umr	0.3	1.37	5791	579	25.9	2.34	1
RESERVOIR	0.23	1.55	6657	665	32.7	2.16	0.91
HAWAR	0.3	6.24	26472	2647	43.7	2.53	1
LEKHWAIR	0.3	7.79	36000	3600	44.6	2.65	1
HITH	0.3	10.87	46000	4600	46.2	2.88	1

Table 3. Simulation schedule

Step	Duration	Operation	No of Wells
1	2020 - 2025	Natural Production	2
2	2025 – 2050	Water Flood 5-Spot pattern	97 producers. 95 infill injectors 26 peripheral injectors
3	2050 – 2080	CO_2 EOR Pilot project at the crest of structure	12 Injectors 12 Producers
4	2080 – 2180	CO_2 sequestration	12 Injectors
5	2180 – 2680	Monitoring of CO2 plume	None

Results

1.Even though the CO2 is injected only in the bottom half of reservoir, within 10 years, the injected CO2 moved up and stopped at the caprock due to buoyancy. CO2 fingering thus occurred through the high permeability top layers to producers, even though these were not perforated in injectors. Figure 6 shows the progression of CO2 mole fraction through at bottom and top layers. In the year 2055, five years after injection, the CO2 is only appearing in the bottom layer thirty-six. But by the year 2060, ten years after injection, the CO2 has already started to migrate to top layer three. There after most of the injected CO2 migrates to top creating the plume just under the caprock. Figure 7 shows the upward movement of CO2 in a cross section.

2.Sensitivity analysis suggests that the amount of CO2 breaking through increases with formation permeability. If the permeability is reduced by four times, almost no CO2 breaks through to producers.

3.The size of CO2 plume became bigger with injection, attaining the maximum size by the end of injection in year 2180. During the five hundred years of monitoring, there is very little change in the CO2 plume size.

4.In the standard case without any rock alteration from injection, it was found that by year 2180, total of 94.01 MTon of CO2 could be injected. Out of which 0.82 MTon of CO2 broke through the high permeable layers and produced at injectors. If the rock is altered and porosity in enhanced the average reservoir pressure by the end of injection also drops by approximately 80 psi. The total CO2 injected in this case increases to 129.3 MTon. The increase is noticed in all three phases of CO2. Figure 8 compares the results of increase in volume for all phases for the two cases.

5.Due to high formation water salinity and low water saturation, only 4% of injected CO2 dissolves in water. Almost 70% stays dissolved in oil and remaining 25% stays in gas phase. The CO2 solubility increases with reduced salinity.

6.On the geomechanics side simulations results are compared for both cases. The geomechanical integrity of the reservoir was found to remain intact. The change in pressures changes the effective stress and the reservoir stress state moves around on the Mohr-Coulomb circle. However, no part of the reservoir or caprock touches the failure line as shown in Figure 9. More complex failure model like cap-failure etc. can be incorporated if the suitable data is available.

7.With production and drop in pressure, the reservoir compacts from the weight of overburden rock. As a result, the overlying rock strata also move down. In both cases the deformation in overburden strata reaches surface causing a subsidence bowl on surface. Figure 10 shows the displacement of reservoir top and surface along the arbitrary line shown in inset for the case of no porosity enhancement. At the end of water flood when the reservoir pressure is the lowest, the reservoir has compacted, and the ground surface has subsided. The top of reservoir has moved down by 1.17 in, and the ground has subsided by 0.2 in relative to edge of reservoir. As the CO2 is injected, the reservoir pressure increases causing it to expand and uplift the top of reservoir and the surface. The reservoir heave by the end of simulation is 0.31 in and the surface uplift is 0.02 in from initial condition.

8.Bigger displacement is observed in case of porosity enhancement near injectors as shown in Figure 11. In the first ten years of CO2 injection, when porosity increases by 10%, the maximum downward movement of reservoir top is 2.68 in, and surface subsidence is 2.51 in. Continuous CO2 injection increases the pore pressure and causes uplift of reservoir top and surface. By the end of injection period in 2180, the ground has uplifted by 0.72 in. During the monitoring period, the uplift gradually subsided to a total of 0.68 in.

Conclusion

The case study shows that the giant carbonate reservoirs in Middle East have good potential to act as a CO2 storage. Due to lying in a low tectonic area and absence of major faults, the stored CO2 has less chance of leaking. The 4-way closed structures, overlain by thick shales and tight carbonates have good potential to act as a seal. The normal life cycle experienced by these fields and CO2 injection is unlikely to cause a

geomechanical breach of loss of containment. If the porosity does enhance due to CO2 alteration, it will enhance the storage capacity. There is a small risk to ground facilities due to ground movement, which can be minimized through INSAR surveillance. Most of the onshore field in the area lye in un-inhabited areas which is conducive for such an operation.

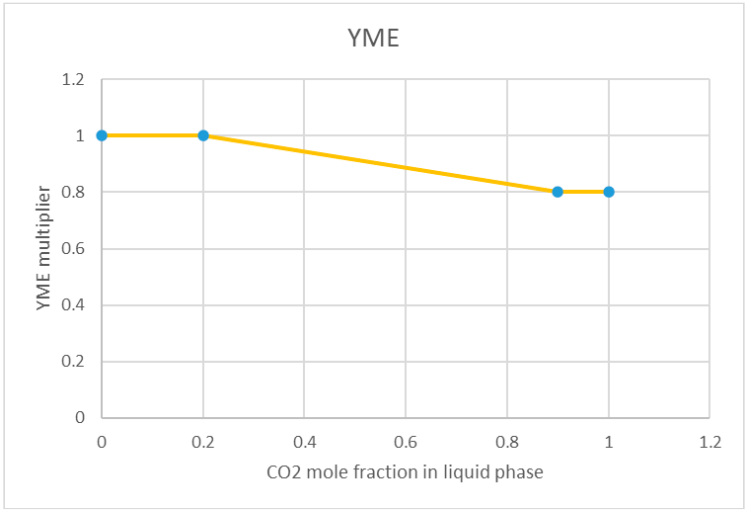

Figure 1. A simple function showing the multiplier used to decrease Young's modulus with CO2 mole fraction.

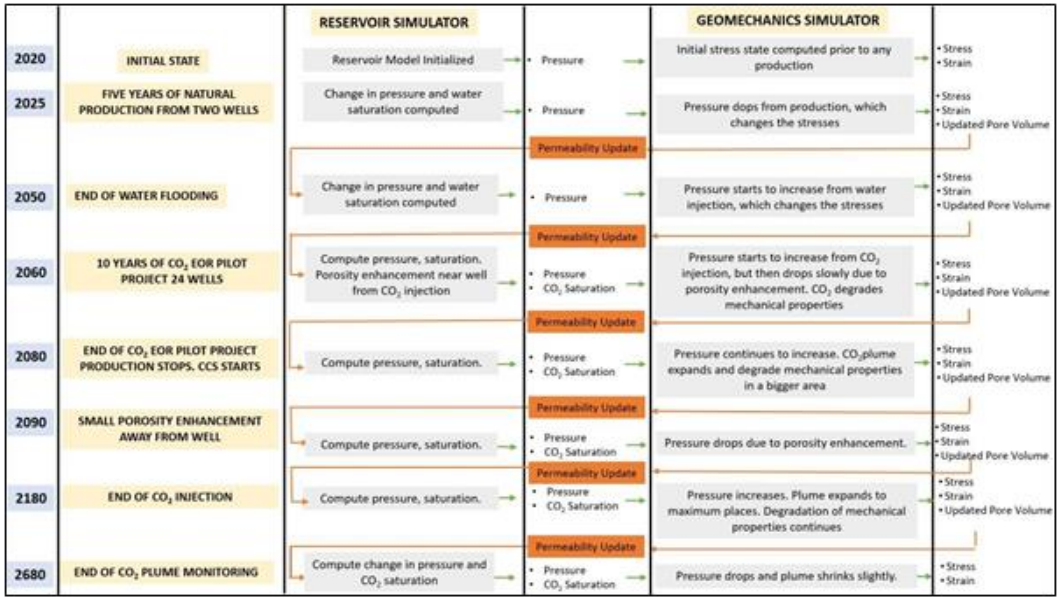

Figure 2. Two-way coupling scheme implemented between reservoir and geomechanics simulators.

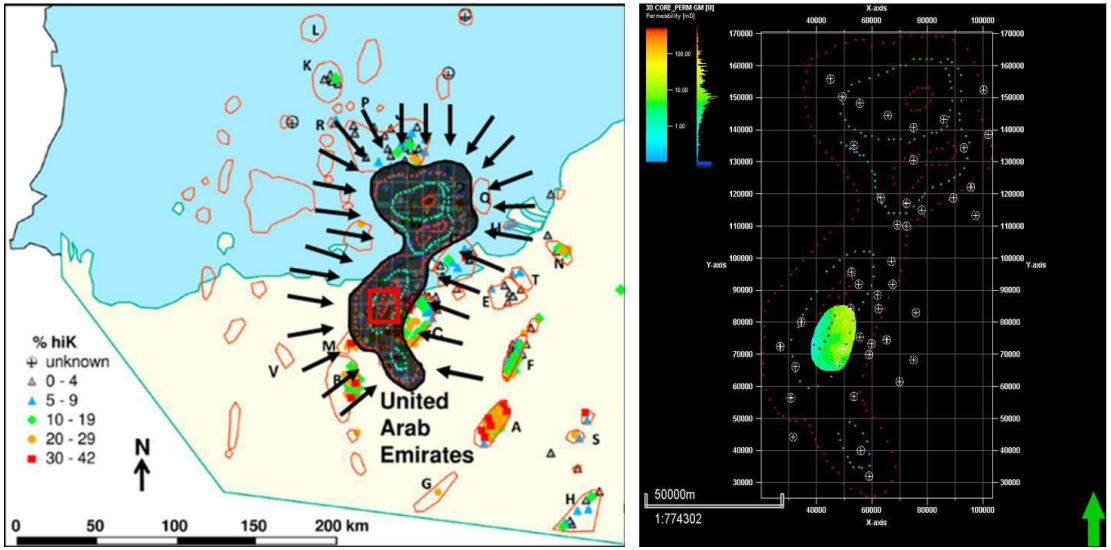

Figure 3. COSTA model and the area where the project is done. Taken from [1].

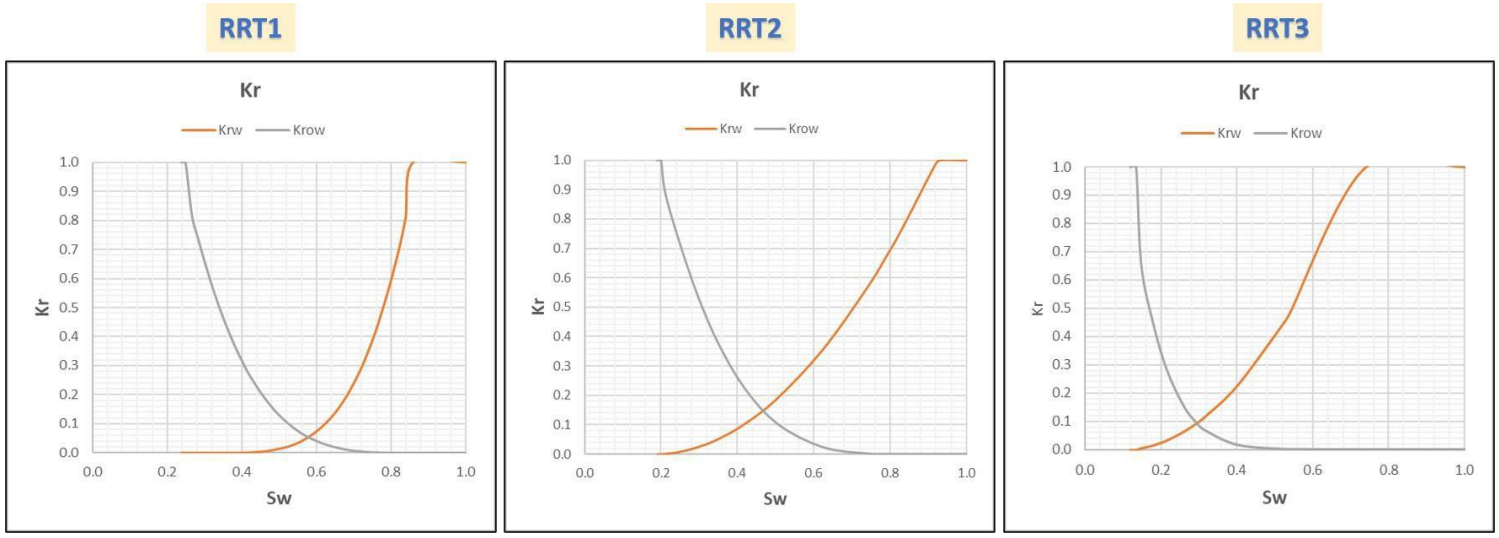

Figure 4. Relative permeability curves of the three Reservoir Rock Types (RRT).

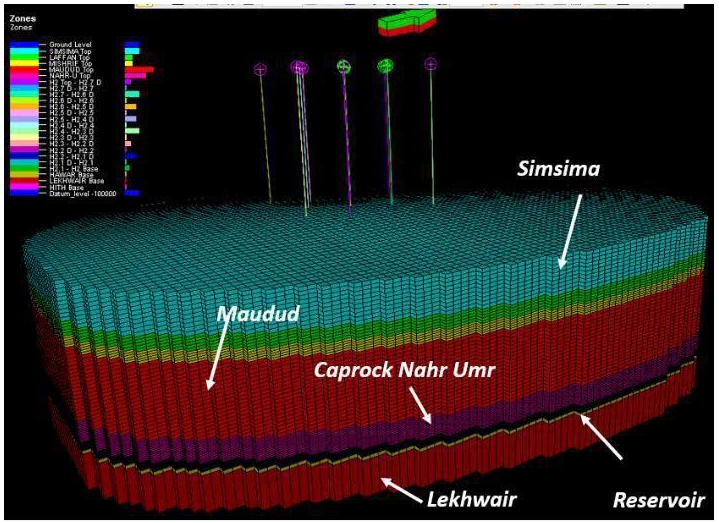

Figure 5. 3D structure of geomechanics simulation.

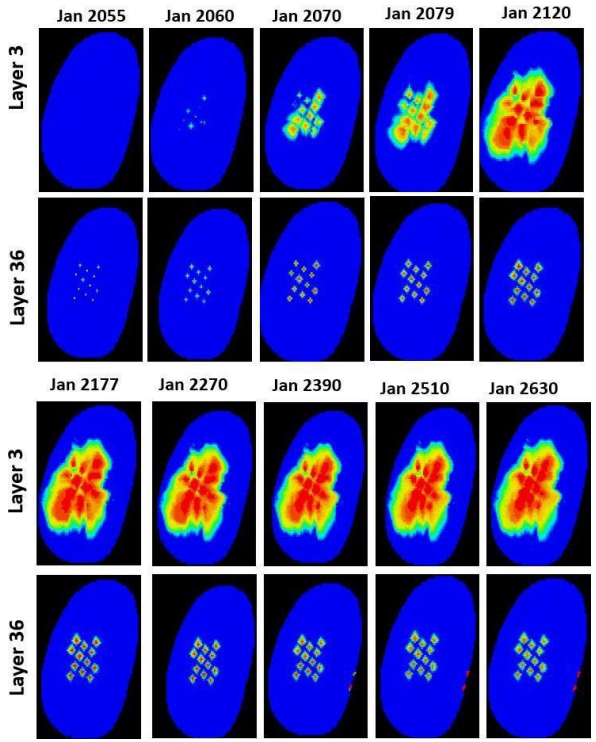

Figure 6. Progression of CO2 mole fraction through time at bottom and top layers.

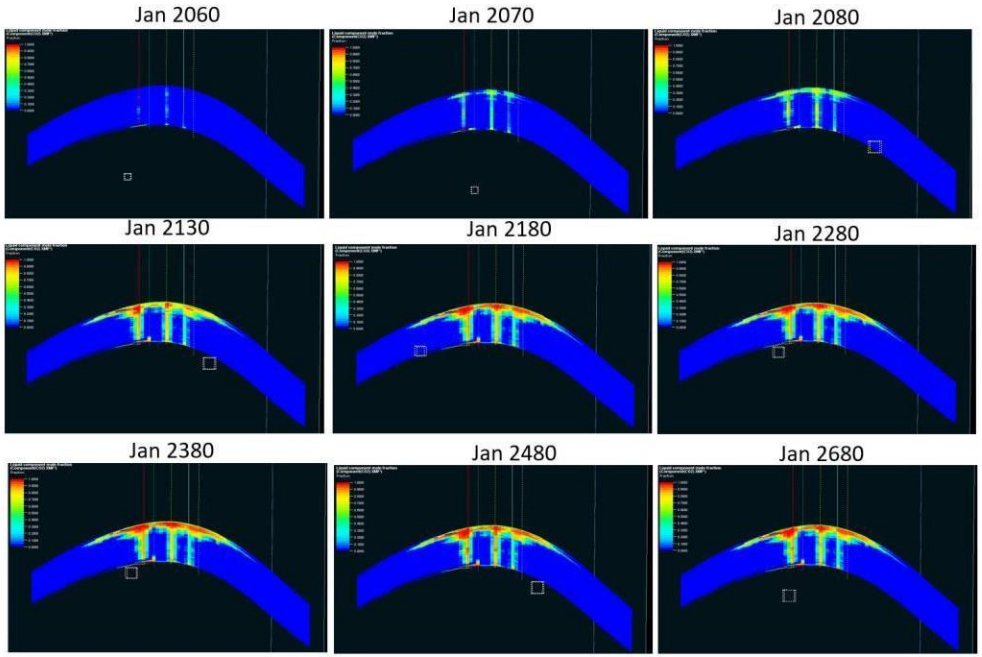

Figure 7. Progression of CO2 mole fraction in liquid phase

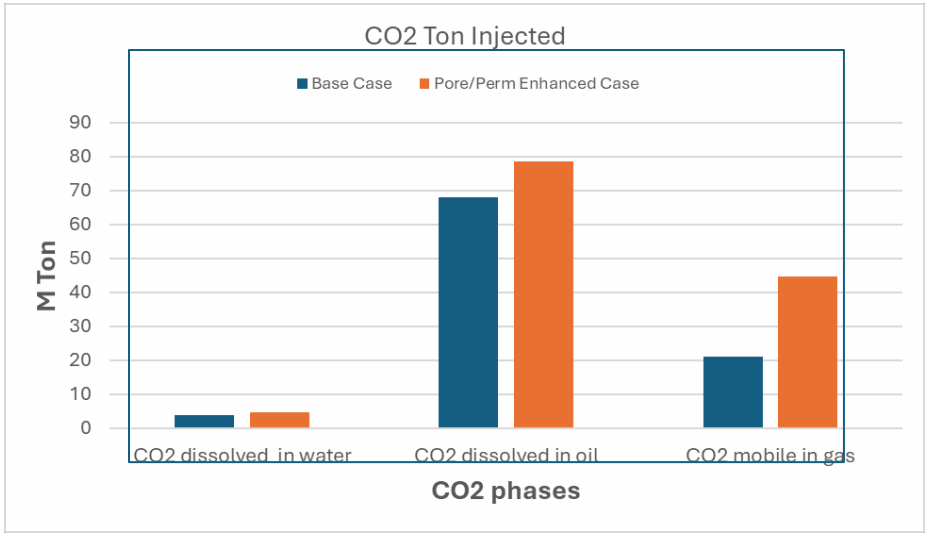

Figure 8. Comparison of CO2 injection results for standard and pore/perm enhanced case.

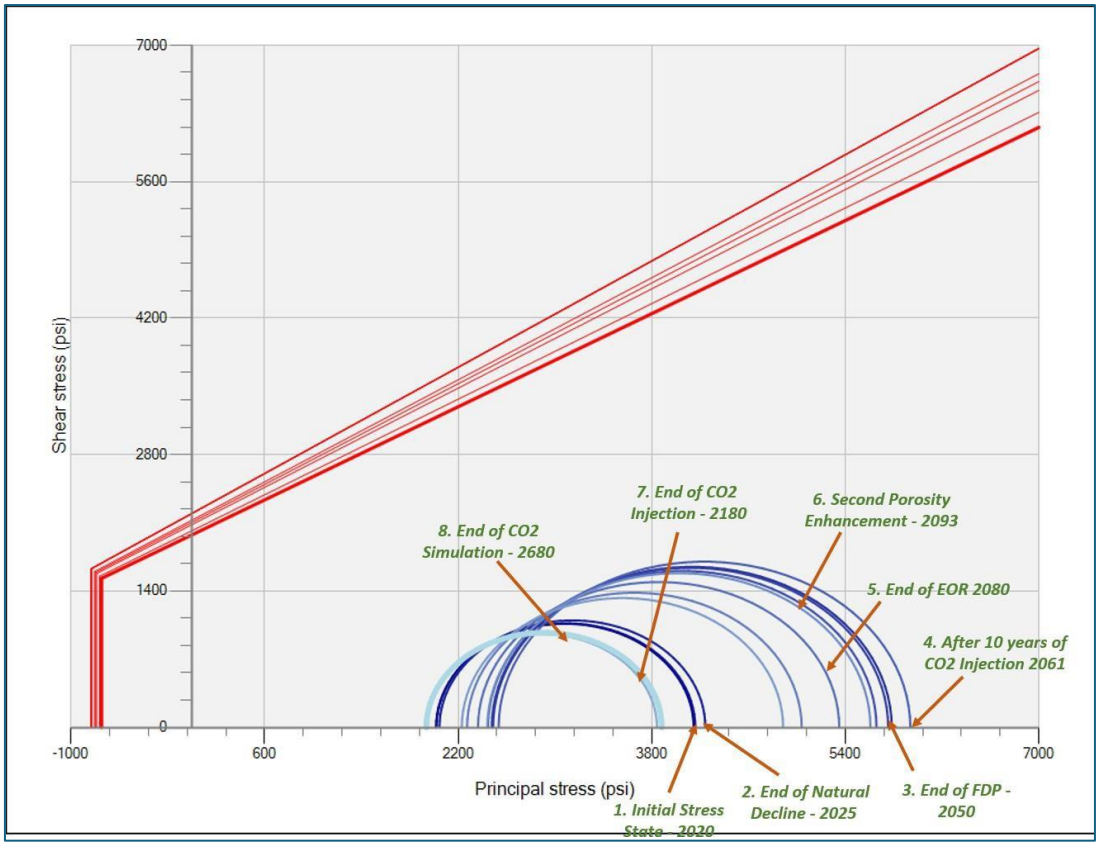

Figure 9. Progression of stress state in a reservoir cell at different time steps for the pore/perm enhancement case.

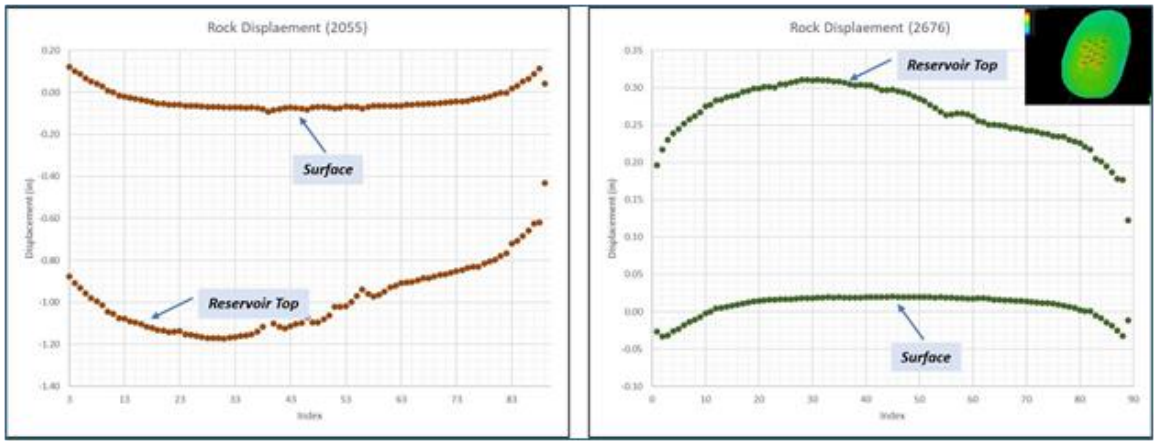

Figure 10. Displacement of ground and reservoir top in 2055 and 2676 from standard case with no porosity alteration, shown along the arbitrary line as in inset.

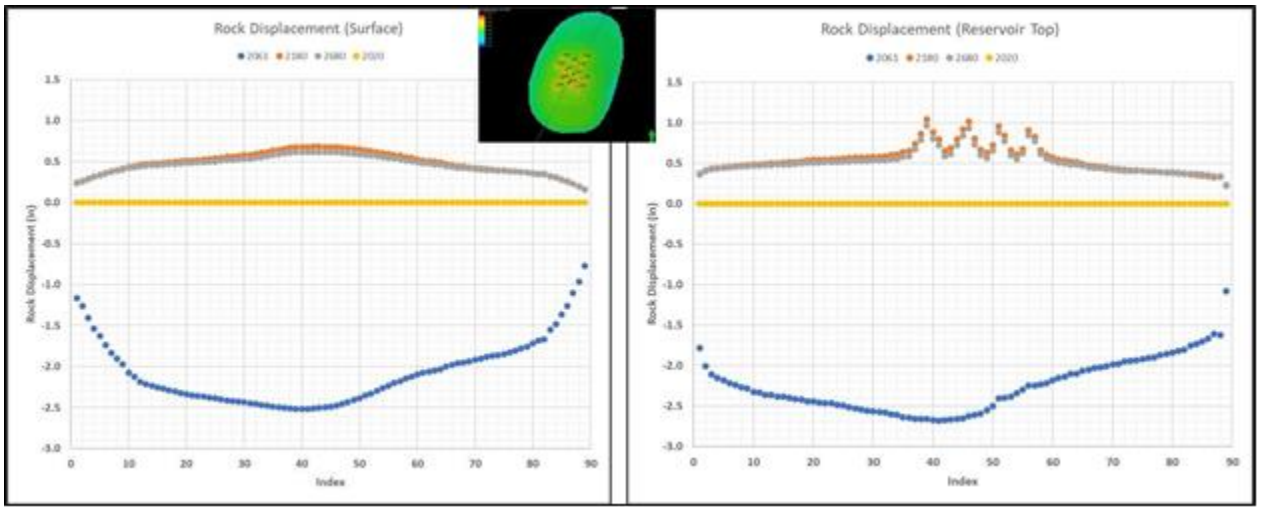

Figure 11. Rock displacement of reservoir top on right and ground on left for the Case of porosity enhancement.

References

1. COSTA Gomes, J., Geiger, S., and Arnold, D., The design of an open-source carbonate reservoir model, Institute of Geoengineering, Heriot-Watt University, UK, Available at: https://pure.hw.ac.uk/ws/portalfiles/portal/60576766/petgeo2021_067.pdf (Retrieved 25-Feb- 2023).

2. Maroto-Valer, M. M., Developments and innovation in CO2 capture and storage technology, Volume 2 (CO2 storage and utilization), (2010), Woodhead Publishing, Table 2.1 and 2.2, Page 31-32, Available at: https://abdn.primo.exlibrisgroup.com/discovery/fulldisplay?docid=alma9917945518905941&context=L&vid=44ABE_INST:44ABE_VU1&lang=en&search_scope=MyInstitution&adaptor=Local%20Search%20Engine&tab=LibraryCatalog&query=any,contains,Developments%20and%20innovation%20in%20CO2%20capture%20and%20storage%20technology&offset=0 (Retrieved 14-Jul- 2023).

3. Zaree, D., Rostami, B., Kostarelos, K., (Jun 2021). Petrophysical changes of carbonate rock related to CO2 injection and sequestration, International Journal of Greenhouse Gas Control.

4. Pokrovsky, O. S., Golubev S. V., Schott, J. and Castillo, A., (2009). Calcite, dolomite, and magnesite dissolution kinetics in aqueous solutions at acid to circumneutral pH, 25 to 150 °C and 1 to 55

atm pCO2: New constraints on CO2 sequestration in sedimentary basins, Chemical Geology 265:20–32.

5. Luquot, L., Rodriguez, O. and Gouze P., (2004). Experimental characterization porosity structure and transport property changes in limestone undergoing different dissolution regimes, Transport in Porous Media 101(3):507–532.

6. Smith, M. M., Sholokhova, Y., Hao Y. and Carroll S. A., (2013). CO2-induced dissolution of low permeability carbonates. Part I: Characterization and experiments, Advances in Water Resources 62:370–387 (2013).

7. Saaltink, M., Vilarrasa, V., Gaspari, F. D., Silva, O., Carrera, J., Rotting, T. S., (2013). A method for incorporating equilibrium chemical reactions into multiphase flow models for CO2 storage, Advances in water resources 431-441.

8. Zaree, D., Rostami, B., Kostarelos, K., (Jun 2021). Petrophysical changes of carbonate rock related to CO2 injection and sequestration, International Journal of Greenhouse Gas Control.

9. Lamy-Chappius, B., Angus, D., Fisher, Q., Grattoni, C. and Yardley, W., (2014). Rapid porosity and permeability changes of calcareous sandstone due to CO2 enriched brine injection, Geophysical research letters, 41.

10. Smith, M., Hao, Y., Spagler, L., Lammers, K., Carroll, S., (2019). Validation of a reactive transport model for predicting changes in porosity and permeability in carbonate samples. International Journal of Greenhouse gas Control 90-102797.

11. Jibar, H. A. I., Aljniebi, N., Al Ali R. H. M., Khan, K. A., Salahuddin A. A., and others, (2020). Pilot wellbore data integration for CO2 / Water Injection and far field tectonic strain calibration (SPE- 202600), Abu Dhabi International Petroleum Exhibition and Conference.